Fuel 404 (2026) 136089

Contents lists available at ScienceDirect

Fuel

journal homepage: www.elsevier.com/locate/fuel

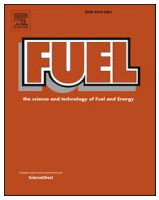

Full Length Article

# Thermal desorption and coke deposition studies of spent zeolite catalysts in the hydrocracking of expanded polystyrene waste

Olajumoke Alabi-Babalola [a,b,**], Vijayalakshmi Thangaraj [a], Nasser Alqahtani [a,d], Hubertus Warsahartana [a], Matthew Smith [a], Edidiong Asuquo [a], Carmine D'Agostino [a,c], Arthur Garforth [a,*]

[a] Department of Chemical Engineering, School of Engineering, Engineering A, University of Manchester, Oxford Road, Manchester M13 9PL, UK
[b] Department of Chemical Engineering, Obafemi Awolowo University, Ile-Ife, Nigeria
[c] Dipartimento di Ingegneria Civile, Chimica, Ambientale e dei Materiali (DICAM), Alma Mater Studiorum – Universita di Bologna, Via Terracini, 28, 40131 Bologna, Italy
[d] King Abdulaziz City for Science and Technology, Saudi Arabia

ARTICLE INFO

*Keywords:*
Chemical recycling
Hydrocracking
Polystyrene
Zeolite catalysts
Thermal desorption
Thermogravimetric analysis
Coke deposition

ABSTRACT

The development of sustainable catalysts towards the chemical recycling of waste plastics has become imperative due to the huge amount of plastic waste generated, the associated disposal problems, and the attendant negative effects on human health and the environment. Spent zeolite catalysts used in the hydrocracking of waste polystyrene have been analysed with focus on coke deposition and product distribution via thermogravimetric analysis and thermal desorption studies respectively. The proton forms of the zeolites (HY and HBeta), the platinum-doped forms obtained via 1 % wt. impregnation: 1PtHY and 1PtHBeta, which were further thermally reduced to $1Pt^0HY$ and $1Pt^0HBeta$ respectively were used for various hydrocracking process reactions. Results showed that the higher catalyst loading in hydrocracking reactions caused a reduction in the amount of coke deposited on the catalyst surface as coke content decreased from 15 to 11 % at a polymer:catalyst of 15:1 and 5:1 respectively. At higher reaction times (60 min), temperatures (330 °C), and pressures (25 bar $H_2$), the amount of coke decreases indicating thermal stability of the porous catalysts under harsh reaction conditions. The presence of platinum significantly reduced the amount of coke formed from 35 % (HY) to 16 % (1PtHY), and from 41 % (HBeta) to 15 % (1PtHBeta) implying that the metal provided high resistance to coking. Repeated catalysts reuse showed the deposition of aromatics on the catalysts surface and a slight increase in the average particle size of the Pt nanoparticle from 3.1 nm for a single run to 4.0 nm for repeated runs using $1Pt^0HBeta$. Thermal desorption analysis revealed the presence of mostly mono-aromatics, indicating that the more condensed polyaromatics desorbed from the zeolite pores undergo cracking reactions leading to the formation of lower molecular weight hydrocarbon molecules, thus giving insights on the nature of hydrocarbon species on used catalysts.

## 1. Introduction

Plastic pollution has been recognised as one of the greatest global environmental problems and it has been predicted that unless action is taken, there will be a three-fold increase in the amount of plastic that flows into the water bodies by 2040 from the current 400 million metric tons of global annual plastic waste generated [1]. The disposal and recycling challenge, coupled with the fact that there are no changes with the production and consumption of plastics has made plastic waste management an urgent global problem. Feedstock or chemical recycling of plastic waste involves the breakdown of the polymer waste in the presence of certain chemical agents to form original monomers or other useful industrial feedstocks [2]. This form of recycling method is generating interest amongst researchers over the last decade as it leads to the generation of value-added products, while diverting from mechanical recycling, landfills and incineration as the world moves toward

* Corresponding author.
** Corresponding author at: Department of Chemical Engineering, School of Engineering, Engineering A, University of Manchester, Oxford Road, Manchester M13 9PL, UK.
*E-mail addresses:* olajumoke.alabi-babalola@manchester.ac.uk (O. Alabi-Babalola), arthur.garforth@manchester.ac.uk (A. Garforth).

https://doi.org/10.1016/j.fuel.2025.136089
Received 6 February 2025; Received in revised form 15 May 2025; Accepted 22 June 2025
Available online 25 July 2025

reducing carbon dioxide emissions [3]. The major chemical recycling protocols include: depolymerisation, gasification, and cracking [2,4,5]. Depolymerisation reactions involve the breaking down of polymer molecules into their respective monomers or oligomers, which can then undergo further polymerisation reactions. Examples of depolymerisation reactions include: hydrolysis, glycolysis, and alcoholysis. However, depolymerisation of addition polymers, which make up 70 % of municipal solid plastic waste [2] are not easily converted into original monomers. Gasification reactions involve the use of heat, controlled steam, oxygen, or air to convert plastics into syngas consisting of a mixture of hydrogen and carbon monoxide, alongside other toxic by-products [6].

On the other hand, cracking of plastic waste could either be by thermal (pyrolysis), catalytic cracking or hydrocracking [7–11]. Pyrolysis involves the use of heat in an inert atmosphere to breakdown the polymeric bonds into a range of gaseous, liquid, and solid molecules [12,13]. Catalytic cracking and hydrocracking are attractive chemical recycling techniques as they produce isomers of lower molecular weight hydrocarbons, often in the presence of bifunctional catalysts having both active metal and acid sites and reactions occuring at moderate reaction temperatures and $H_2$ pressures. It is a form of feedstock recycling currently being explored by plastic recyclers as it produces different boiling point ranges of hydrocarbon fuels which are valuable in the refinery industry. Hydrocracking on bifunctional catalysts is quite significant in polymer recycling and petroleum refining as it helps to convert heavy molecular weight hydrocarbons such as heavy vacuum gas oil (VGO) into diesel and light oils which can be used as jet fuels [14]. The reaction pathway is versatile as it can be subjected to different process variants, which allows for specific needs or requirements in the refinery stream to be met, thus giving a broad range of quality products.

Bifunctional catalysts have been used by several authors [15–21] to process a wide range of polymer feedstock. Trueba et al. [22] used Pt/Pd/zeolite Y catalyst in the hydrocracking of a mixture of PS blended with VGO using a batch reactor at operating conditions: 380–420 °C, 80 bar $H_2$ to obtain a wide range of liquid products containing light cycle oil and naptha which can be blended for automotive fuels. Different forms of Pt-modifed zeolites were used by David et al. [23] in the ring-opening reactions of decalin, in which case the presence of Pt also promoted isomerization and the ring opening rates were 5 times higher compared to the proton-form of the zeolites. Vance et al. [18] used a Pt-tungstated zirconia in the hydrocracking of LDPE to promote isomerization reactions leading to the production of highly valued branched fuels and alkanes that were suitable for use as lubricants. The nature of the final degradation products formed depends on the number of carbon atoms in the reactant alkane molecule, the type of scission reactions, the steady state concentration of the intermediates obtained from the reactant molecule, the extent and the rate of competitive adsorption/desorption mechanism. This general principle applies to hydrocracking reactions of any polymer molecule in the presence of bifuntional catalysts [24].

However, the performance of hydrocracking in the chemical transformation of plastic waste into different hydrocarbon streams and residue brings about the issue of catalyst deactivation which is attributed to a lot of factors such as attrition [25,26], metal or coke deposition [27,28]. One of the factors that causes deactivation of catalysts used in hydrocracking is coke deposition [29,30] and different methods such as FTIR [22], thermogravimentary differential thermal analysis (TG-DTA) [31], UV-Raman spectroscopy [31], and temperature-programmed oxidation (TPO) [32], have been used to determine the nature and quality of the coke content. Coke formation in hydrocracking reactions occurs when the degraded molecules continually produce sediments on the catalyst surface. These sediments undergo different chemical changes and aggregate via Van der Waals interactions to form species commonly regarded as coke either on the external surface of the catalyst (external coke) or within the catalytic channels (internal coke) [22]. Coke deposits are largely influenced by a number of factors such as nature of the feedstock [32,33], the catalysts' properties [34], and the reaction operating conditions [29,31]. The use of conventional noble metals such as platinum and paladium [35–37] has helped in the elucidation of the deactivation mechanisms. However, an in-depth understanding of the coking process and coke characterisation would help to improve catalysts performance and assess catalyst regeneration technology. This is also expected to optimise and enhance existing industrial catalytic processes.

This work involved the characterisation of coke deposited on the surface of platinum-doped zeolite HY and zeolite Beta catalysts during the hydrocracking of post-consumer polystyrene (PS) waste, while also investigating the effects of metal impregnation and hydrocracking reaction conditions of temperature, time, hydrogen pressure, and polymer: catalyst ratio on coke deposition. In addition, an extensive study of the spent catalysts after several repeated hydrocracking runs has been carried out to understand the extent of catalyst decay, nature and composition of coke, as well as the effect of coke on hydrogenation/dehydrogenation reactions.

## 2. Materials and methods

### 2.1. Catalyst preparation and hydrocracking process

Two sets of catalysts were used in this study HY and HBeta, and were impregnated with 1 % wt. of platinum in the form of $Pt(NH_3)_4Cl_2{\cdot}xH_2O$ The salt was dissolved in deionized water at room temperature and left to stir at 50 °C for about 8 h with a stirring speed of 500 rpm to ensure proper dispersion of the metal on the catalyst support until the solution forms a thick paste. Afterwards, the catalysts were dried in the oven at 110 °C, and further calcined in air at 550 °C for 5 h at a ramp rate of 5 °C/min to allow decomposition of the platinum salt [38]. Catalyst reduction was carried out using a tubular reactor by heating the catalyst pellets (250 −600$\mu m$) from ambient temperature to 400 °C/min at a hydrogen flow rate of 5 mL/min, heating rate 10 °C /min for 4 h.

The catalysts were used in the catalytic hydrocracking of PS using a 300 mL stainless steel batch Parr reactor which is attached to an inlet stirrer. Both polymer and catalyst were loaded into the reactor under the flow of hydrogen gas and different operating conditions were varied: reaction temperature (300 –330 °C), reaction pressure (15 – 25 bar $H_2$), reaction time (15, 60 min), and polymer:catalyst ratio (5:1, 10:1, 15:1). At the end of each hydrocracking experiment, gas and liquid products were collected, and the coke residue was obtained after drying the reactor at 200 °C to remove any residual liquid that might be stuck to the reactor walls. Spent catalysts were reused for four repeated hydrocracking runs at 330°C, 60 min, 20 bar $H_2$, at an initial polymer:catalyst ratio of 10:1.

Three different forms of the parent zeolite are reported namely: HY and HBeta representing the parent zeolite, the oxidised form of the Pt-doped catalysts designated as: 1PtHY and 1PtHBeta, and the reduced forms denoted as: $1Pt^0HY$ and $1Pt^0HBeta$. These catalysts are used for different hydrocracking reactions at varying parameters earlier mentioned and the spent catalysts are further characterised in this study.

### 2.2. Catalysts and coke characterisation

The acidity profile of the fresh catalysts were determined using ammonia-temperature-programmed desorption ($NH_3$-TPD) with the Microtrac MRB Belcat II Catalyst Analyzer. The catalysts were first pretreated with Ar at 600 °C for 30 min and subsequently cooled to room temperature. Afterwards, the samples were heated to 800 °C with 2 % $NH_3$ at a ramp rate of 10 °C /min. XPS measurements on zeolite samples were carried out using an X-ray photoelectron spectrometer (XPS; Kratos AXIS Ultra DLD), equipped with monochromated Al Kα radiation as an X-Ray source (1486.6 eV), a charge neutralizer, and a hemispherical electron energy analyser. The XPS spectra were processed using Casa XPS (Version 2.3.19PR1.0). All samples were calibrated with respect to the adventitious carbon 1 s peak at 284.8 ev [39,40]. The pore

distribution of catalysts were determined via BET analysis and nitrogen sorption isotherms were recorded on a BET Micrometrics ASAP 2060 instrument. The catalysts were first degassed at 400 °C for 3 h and subsequently analysed using liquid nitrogen 77 K to obtain the surface area and pore characteristics.

Coke characterisation and analysis was carried out using thermogravimetric analysis (TGA), Fourier transform infrared spectroscopy (FTIR), high-angle annular dark-field scanning transmission electron microscopy (HAADF-STEM), and thermal desorption-GC–MS (TDS-GC–MS) analysis. The thermal degradation profile of the spent catalysts was carried out using a TGA Q5000 (TA instrument). The coke residue was obtained by heating about 5 mg of the coke sample under an inert nitrogen atmosphere from ambient to 600 °C at a ramp rate of 10 °C /min and kept isothermal for 60 min intermittently at different temperatures of 200, 400, and 600 °C following which the atmosphere was switched to air for another 60 min. The amount of coke in the residue was obtained as the difference between the weight loss in nitrogen and that of air **(Equation (1)**, such that:

$$Amount\ of\ coke(\%) = \frac{w_1 - w_2}{w_1} \times 100 \quad (1)$$

where $w_1$ and $w_2$ represents the weights of residue (mg) after decomposition under nitrogen gas and air respectively.

The chemical structure and functional groups of the polymer and catalysts were characterized using FTIR Bruker Vertex 70 over a range of 4000 – 400 $cm^{-1}$. The surface morphology and elemental compositions of the catalysts were analysed with a FEI Quanta 250 FEG. STEM and EDX spectrum images were obtained with an FEI Talos F200X microscope equipped with an X-FEG electron source and Super-X SDD EDS detectors. The experiment was performed using an acceleration voltage of 200 kV and a beam current of approximately 200 pA. The STEM images were acquired with a HAADF detector.

The nature and content of the spent catalysts was determined by use of a thermogravimetric analyser followed by thermal desorption using an Agilent GC-MSD system (Agilent Technology, Santa Clara, US). About 5 mg of the sample was first heated from 25 °C to 700 °C for 30 min with a ramp rate of 10 °C/min with TGA instrument (TGA Q5000). The gases released during the reaction were collected in a tenax absorption tube, which was sealed with brass storage caps to prevent sample contamination before loading into the thermal desorber. Subsequently, the tube was desorbed at 320 °C for 5 min using nitrogen gas at a flow rate of 50 mL/min. The purged gas was temporarily stored in a 30 °C cold trap, then degassed at 320 °C for 3 min and transferred to an Agilent 7980A GC fitted with an Agilent HP-5MS 5 % Phenyl Methyl Siloxane column (30 m × 250 μm × 0.25 μm). The GC was coupled to an Agilent 5975 MSD single quadrupole mass spectrometer in electron ionisation mode (scanning a range of *m/z* 50 to 650 at 2.7 scans/sec; ionisation energy: 70 eV) with helium as the carrier gas. The heated GC interface was set at 280°C, the EI source at 230°C, and the MS quadrupole at 150 °C. The desorption oven temperature was programmed from 40 °C (held for 4 min) to 200 °C at 8 °C/min and held at this temperature for 3 min to give a total run time of 27 min.

## 3. Results and discussion

### 3.1. Catalysts characterisation results

BET analysis revealed a type II isotherm [41]for the zeolite catalysts with the hysteresis steps at $P/P^0 = 0.5 – 0.95$ indicating the presence of mesopores [42] as shown in Fig. 1**a,** with $1Pt^0$HBeta having a higher mesopore volume (0.4 $cm^3/g$) compared to $1Pt^0$HY (0.08 $cm^3/g$). The surface areas were found to decrease after hydrocracking reactions from 521 $m^2/g$ ($1Pt^0$HBeta) to 231 $m^2/g$ ($1Pt^0$HBeta_Single run); and from 536 to 112 $m^2/g$ for $1Pt^0$HY and $1Pt^0$HY_Single run respectively. The significant reduction in the surface areas and pore sizes of the spent catalysts is due to the deposition of the condensed coke precursors on the catalytic surface during and after hydrocracking reactions. Two different acid sites are identified from the TPD thermograms **(**Fig. 1**b)** corresponding to weak and strong acid sites [43,44]. The weak acid sites are in the region between 40 – 300 °C with a maxima at about 130°C, while the strong acid sites were obtained between 450 – 700 °C with maxima at about 590°C. The presence of the strong acid sites upon platinum doping is expected to influence hydrocracking reactions.

Al 2p and Pt 4f XPS diffraction analysis of $1Pt^0$HY **(**Fig. 2**a)**and $1Pt^0$HBeta **(**Fig. 2**b)** revealed the presence of both Al and Pt chemical environments. Peak deconvolution showed Al $2p_{3/2}$ and $2p_{1/2}$ BE states at 74.6, 75.1 eV for $1Pt^0$HY and 75.4 and 75.8 eV for $1Pt^0$HBeta respectively, with a doublet splitting of 0.42 eV. These Al BE states corresponds to differently coordinated aluminium states (AlOH) and Al-fold sites of the zeolite framework [45,46]. In addition, the asymmetric $4f_{7/2}$ and $4f_{5/2}$ spectra of $1Pt^0$HBeta, separated by a constraint of 3.35 eV were deconvoluted at 71.9 and 75.3 eV which is attributed to the metal form of Pt ($Pt^0$) and consistent with values obtained in literature [47]. Similar values were obtained for $1Pt^0$HY at 71.1 and 74.5 eV for core levels $4f_{7/2}$ and $4f_{5/2}$, with an intensity ratio of a factor of 0.75 [48].

### 3.2. TGA quantitative analysis of coke

The mechanism of coke formation on the catalyst surface is explained by the inability of the catalyst to continuously crack the polymer chains

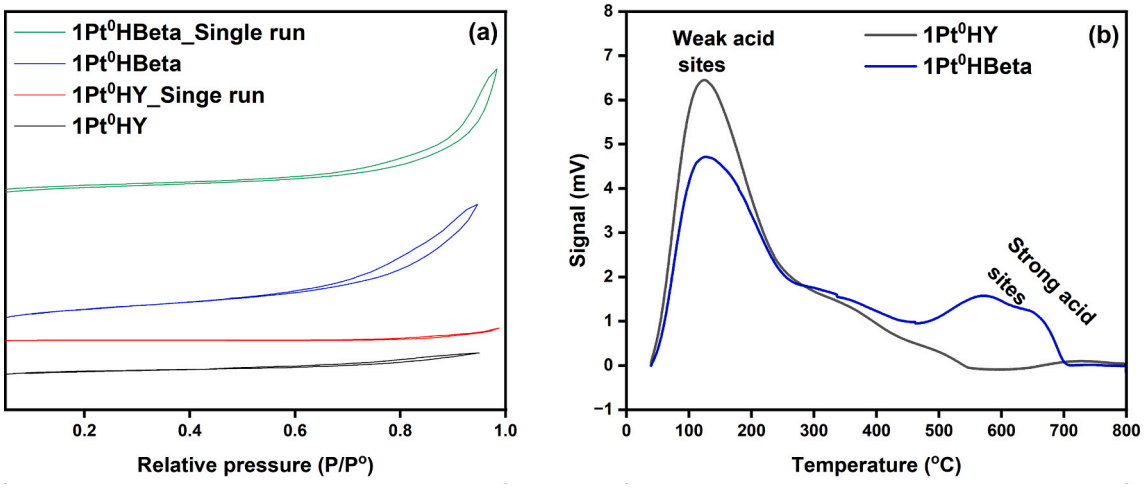


**Fig. 1.** (a) $N_2$ adsorption isotherms of fresh and spent zeolite catalysts (b) Acidity profiles of fresh catalysts before hydrocracking reactions.

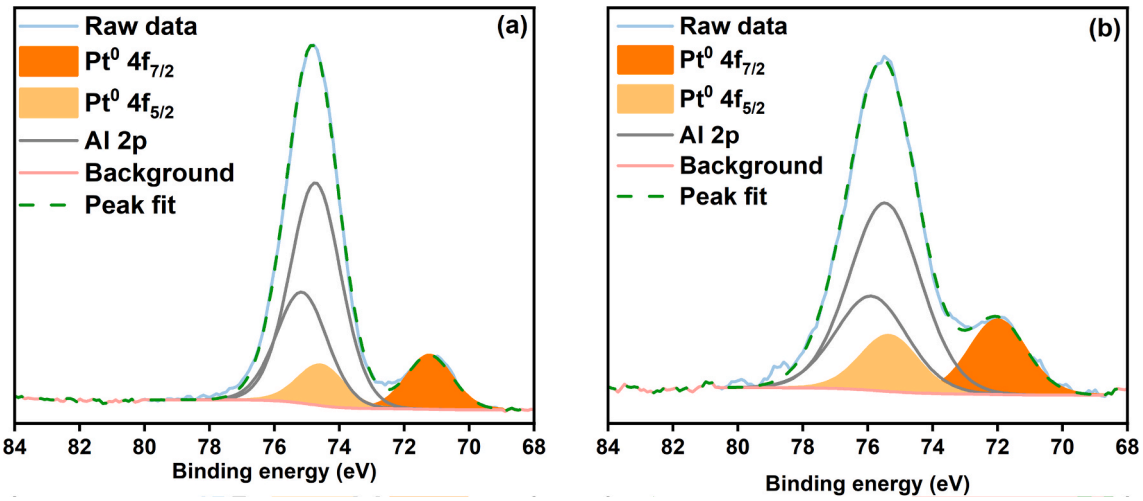


**Fig. 2.** XPS Al 2p and Pt 4f spectra of fresh catalysts (a) $1Pt^0HY$ (b) $1Pt^0HBeta$.

as reaction progresses leading to partially degraded PS molecules in solution [22], thus, producing deposits on the catalyst surface. The deposits further undergo different forms of transformations such as those caused by Van der Waals forces of interactions resulting in alteration in their compositions to form nanoaggregates commonly regarded as coke. The thermal degradation profiles of fresh unspent catalysts: $1Pt^0HY$, and different spent catalysts: parent zeolite (HY), Pt-doped oxidised HY (1PtHY), Pt-doped reduced form for a single hydrocracking run ($1Pt^0HY\_Single$ run) and Pt-doped reduced form for four repeated hydrocracking runs ($1Pt^0HY\_Recycled$ run 4) are shown in Fig. 3, while those of HBeta catalysts are represented in Fig. 4.

The area to the left region of the black dashed vertical line represents the region under nitrogen atmosphere, while the area to the right region is the region under air. The change in the atmosphere is because coke is carbon and thus, will not decompse within the nitrogen atmosphere. Under nitrogen atmosphere, all the volatile components must have completely decomposed such that when the system is switched to an oxidising atmosphere (air), the coke which is carbonaceous in nature will readily convert to carbon dioxide thereby exiting the TGA pan as coke. The spent catalysts were used at identical operating conditions of 330°C, 60 min, 10:1 polymer:catalyst ratio, and at 20 bar $H_2$. The TGA profile of the fresh catalysts ($1Pt^0HY$ and $1Pt^0HBeta$): in red dotted lines

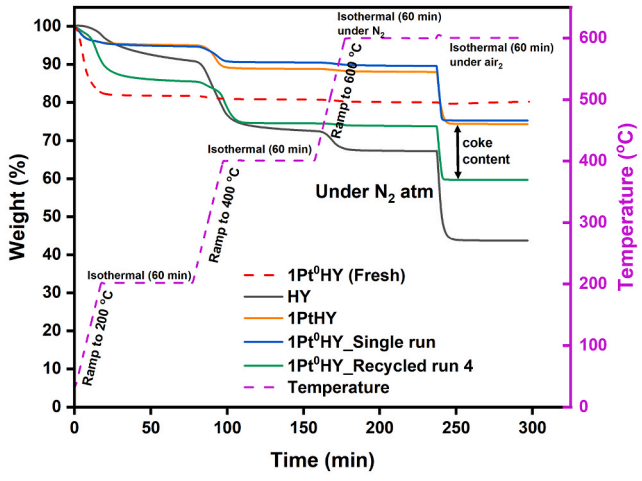


**Fig. 3.** Schematic representation of TGA analysis for coke content determination for fresh and different spent HY catalysts used for polystyrene hydrocracking reactions (dashed black line provides guide to the eye separating nitrogen gas and atmospheric air regions).

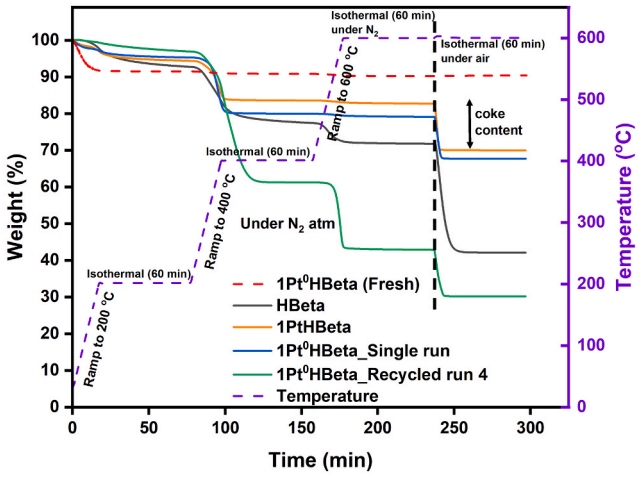


**Fig. 4.** Schematic representation of TGA analysis for coke content determination for fresh and different spent HBeta catalysts used for polystyrene hydrocracking reactions (dashed black line provides guide to the eye separating nitrogen gas and atmospheric air regions).

showed that there are no coke present prior to hydrocracking as constant weight was observed both under nitrogen and air.

The reused catalysts showed three (3) different stages involving mass change namely: 25 – 400, 400 – 600 °C under $N_2$, and 600 °C under air. The weight loss associated with the first stage is related to moisture, the second stage is related to decomposition of some physical sorbents and volatile organic compounds, while the third stage represents the amount of coke present [49].

Reactions involving the parent zeolite (HY and HBeta), and the oxidised forms of the Pt-doped catalysts (1PtHY, 1PtHBeta) have coke, often regarded as "hard coke" [49] as their main coke components, due to thermal ageing. This implies that the reduced forms of the Pt-doped catalysts ($1Pt^0HY$, $1Pt^0HBeta$) have higher activity and stability compared to the oxidised forms. It is worthy to note that the hard coke content obtained represents the summation of both internal and external coke of the spent catalysts. The internal coke is that formed in the zeolite channels attributable to the condensation reactions of olefins to form polyaromatic hydrocarbons (PAHs) through condensation, isomerization, or cyclization [32]. The external coke represents those deposits located on the external surface of the catalyst and is attributable to coke structures with less condensation degrees that requires lower operating temperatures.

**Table 1**
TGA weight loss compositions of spent ZHY catalysts used for hydrocracking of expanded post-consumer polystyrene waste.

| Polymer feedstock/catalyst | Varied parameter | Weight loss % | | |
|---|---|---|---|---|
| | | Moisture content | Physical sorbents (under $N_2$) | Coke content: isothermal at 600 °C (under air) |
| HY/330 °C /60 min/10:1/20 bar $H_2$ | HY | 9 | 26 | 35 |
| 1PtHY/330 °C /60 min/10:1/20 bar $H_2$ | 1PtHY | 5 | 7 | 16 |
| **Pressure series (1Pt$^0$HY)** | | | | |
| 330 °C /15 min/10:1 | 15 bar | 18 | 31 | 19 |
| 330 °C/15 min/10:1 | 20 bar | 13 | 55 | 18 |
| 330 °C/15 min/10:1 | 25 bar | 5 | 50 | 18 |
| **Temperature series (1Pt$^0$HY)** | | | | |
| 60 min/10:1/20 bar $H_2$ | 300 °C | 3 | 46 | 18 |
| 60 min/10:1/20 bar $H_2$ | 315 °C | 5 | 59 | 19 |
| 60 min/10:1/20 bar $H_2$ | 330 °C | 5 | 38 | 17 |
| Recycled run 4 60 min/10:1/20 bar | 330 °C | 15 | 14 | 19 |
| **Polymer:catalyst ratio (1Pt$^0$HY)** | | | | |
| 330 °C /60 min/20 bar $H_2$ | 5:1 | 4 | 18 | 17 |
| 330 °C /60 min/20 bar $H_2$ | 10:1 | 5 | 38 | 17 |
| 330 °C /60 min/20 bar $H_2$ | 15:1 | 3 | 42 | 18 |

There is an approximately 12 % decrease in the coke content in 1PtHY relative to HY **(see** Fig. 3**)**, which is mainly attributed to the difference in the strength and nature of the acid sites of the zeolite catalysts. 1PtHY is less dense in terms of acid sites compared to HY, as such the tendency of the coke precursor species to strongly adsorb on the catalyst acid sites via condensation, oligomerization, or hydrogen transfer reactions is reduced. Similar results were obtained by Fals et al. in their report on the catalytic cracking of vacuum gas oil over zeolite catalysts [32]. The slight increase in the coke content in the spent recycled catalysts: 1Pt$^0$HY_Recycled run 4 (19 %) relative to the spent single run: (1Pt$^0$HY_Single run (17 %) indicated the deposition of more PAHs on the catalyst leading to decay as the catalyst was continually reused for subsequent hydrocracking reactions. The highest amount of coke ( 35 %) was found on the zeolite catalyst with no metal sites (HY) which implies that the absence of an active metal site that provides the hydrogenation function for the zeolite catalyst make its pores more susceptible to the formation of more condensed coke as the coke precursor species continually builds up on the zeolite surface.

The spent parent zeolite HBeta has the highest amount of coke (41 %) due to the high amount of partially degraded polymer molecules that is deposited on the catalysts particles which sequentially covers the active sites and causes pore blockage [50]. This is also caused by the oligomerization and condensation reactions of the olefins and PAHs **(see** Fig. 4**)** respectively occurring at the acidic centres of the zeolite in the absence of the hydrogenating metal [34]. The reduced form of the modified catalyst 1PtHBeta_Single run has a lower amount of coke (14 %) compared to its oxidized form 1Pt$^0$HBeta (15 %), apparently due to its faster polymer degradation ability which produces less amounts of aromatics and more ring opening and hydrogenation products occurring as a result of its activation. The significantly lower amount of coke of the spent Pt-doped catalysts (14 – 15 %) relative to the parent zeolite (HBeta) (41 %) further confirms that the presence of metallic sites prevents blockage of both micro- and mesopores of the catalysts, preventing coke precursor formation, and thus, delays coking. This is in agreement with the results reported by Kubicka et al [23] where they studied the extent of catalyst deactivation on both proton-form and Pt-form of different zeolites in ring opening reactions of decalin. In the case of the recycled catalyst, the amount of coke after four repeated runs is obtained as 29 % which is caused by the increasing partial degradation of PS molecules which continuously poison the metal sites causing catalyst deactivation [22].

Thus, the results obtained strongly suggests that the factors that influence the nature and amount of coke deposition are mainly the zeolite properties largely influenced by its acid strength and hydrogenation ability.

Fals et al. [32] reported that the amounts and nature of coke deposits depends on certain factors such as the nature of feedstock, process conditions, as well as the properties of the zeolite catalysts. The thermal degradation contents of other used catalysts for different process conditions are shown in Tables 1 and 2, while the amounts of coke were calculated using **Equation (1)**.

The used catalysts undergo different heating regimes and the different contents consisting of moisture, organic and inorganic matter were evaluated. The spent catalysts have volatile compounds as the major component with weight loss in the range of 9 – 59 %. The only exception is in the case of 1Pt$^0$HBeta at 330 °C /60 min/20 bar $H_2$/5:1 where the amount of moisture and organic volatiles were obtained as 6 %. The moisture contents of the spent catalysts were mostly negligible with values between 4 – 9 % except for those reactions occurring at lower operating conditions of 15 min (13 % for 1Pt$^0$HY and 19 % for 1Pt$^0$HBeta), and at 15 – 20 bar $H_2$.

The thermal degradation profiles at different hydrocracking reactions of the spent catalysts are represented in **Figs. S2** (mass-dependent reactions)**, S3** (pressure-dependent reaction), and **S4** (temperature-dependent). Similar coke contents (17 – 18 %) were obtained for the pressure-dependent, temperature-dependent, and catalyst concentration-dependent hydrocracking reactions involving 1Pt$^0$HY (Table 1**).**

For HBeta catalysts at constant temperature and time, the coke content was found to decrease as reaction pressure increases with values 19, 18, and 12 % at 15, 20, 25 bar $H_2$ respectively. The spent catalyst at 25 bar was relatively stable at lower degradation temperatures and time, as much lighter products were formed during its hydrocracking reactions compared to those of 20 and 15 bar, which explains the trend at the beginning of the degradation profile, up to ~ 390 °C **(Fig. S3)**. Also, the amount of coke decreases with an increase in reaction temperature with values of 18, 15, and 14 % at 300, 315, and 330 °C respectively at constant reaction time and pressure. The decrease in coke was also observed from 18 to 14 % as reaction time increases from 15 to 60 min.

The decrease in the values of coke as reaction pressure, time, and temperature increases is characteristics of the nature of the acid sites of the zeolite. The mesoporous nature and high strength of the acid sites prevents the coke precursor species from strongly adsorbing continuously onto the zeolite and within the zeolite channels at higher process

**Table 2**
TGA weight loss compositions of spent HBeta catalysts used for hydrocracking of expanded post-consumer polystyrene waste.

| Polymer feedstock/catalyst | Varied parameter | Weight loss % | | |
|---|---|---|---|---|
| | | Moisture content | Physical sorbents (under $N_2$) | Coke content: isothermal at 600 °C (under air) |
| HBeta/330 °C /60 min/10:1/20 bar $H_2$ | HBeta | 7 | 23 | 41 |
| 1PtHBeta/330 °C /60 min/10:1/20 bar $H_2$ | 1PtHBeta | 6 | 12 | 15 |
| **Pressure series (1Pt$^0$HBeta)** | | | | |
| 330 °C /15 min/10:1 | 15 bar | 19 | 53 | 19 |
| 330 °C /15 min/10:1 | 20 bar | 16 | 21 | 18 |
| 330 °C /15 min/10:1 | 25 bar | 4 | 21 | 12 |
| **Temperature series (1Pt$^0$HBeta)** | | | | |
| 60 min/10:1/20 bar $H_2$ | 300 °C | 6 | 33 | 18 |
| 60 min/10:1/20 bar $H_2$ | 315 °C | 4 | 42 | 15 |
| 60 min/10:1/20 bar $H_2$ | 330 °C | 5 | 17 | 14 |
| Recycled run 4 60 min/10:1/20 bar | 330 °C | 3 | 56 | 29 |
| **Polymer:catalyst ratio (1Pt$^0$HBeta)** | | | | |
| 330 °C /60 min/20 bar $H_2$ | 5:1 | 6 | 6 | 11 |
| 330 °C /60 min/20 bar $H_2$ | 10:1 | 5 | 17 | 14 |
| 330 °C /60 min/20 bar $H_2$ | 15:1 | 4 | 19 | 15 |

conditions, thus; delaying catalyst deactivation and coking. However, the amount of coke increases from 11, 14, and 15 % as polymer: catalyst ratio increases from 5:1, 10:1, and 15:1 respectively; *i.e* there is a low amount of coke formed when higher amount of catalyst is used. This implies that the sintering of Pt species takes place during hydrocracking reactions that involves low amount of catalysts (15:1), thus resulting in lower activity due to minimal amount of active sites [51]. Expectedly, the presence of high amounts of catalyst relative to the polymer feedstock in the reaction medium increases the gas yield via enhanced hydrogenation and ring opening reactions thereby inhibiting reactions that lead to coke formation.

### 3.3. Nature of coke formed

The nature of the coke was determined via FTIR analysis of two spent catalysts for single run experiment: 1Pt$^0$HY_Single run, 1Pt$^0$HBeta_Single run) and two spent catalysts for repeated recycled runs: 1Pt$^0$HY_Recycled run 4, 1Pt$^0$HBeta_Recycled run 4 with identical hydrocracking conditions (330°C, 60 min, 20 bar $H_2$). The spectra were collected over a range of 4000 – 400 cm$^{-1}$ as shown in Fig. 5**a and b.** The FTIR spectra of both fresh and spent zeolite catalysts have vibrational frequencies at 1630 cm$^{-1}$ corresponding to a C=C olefin stretching vibration. There are no significant differences between the fresh and spent catalysts of the single runs, indicating there is no catalyst decay or decrease in catalyst activity after the first hydrocracking run. However, spectral differences were observed in the spent catalyst with a single run in which vibrational frequencies are seen in the fingerprint region at 1494 and 1452 cm$^{-1}$ which are attributed to C=C aromatic vibrations [52] confirming the deposition of aromatic carbonaceous compounds. The recycled catalysts (1Pt$^0$HY_Recylced run 4 and 1Pt$^0$HBeta_Recycled run 4) showed more intense peaks at the previously described fingerprint region and at 1630 cm$^{-1}$. It also has distinguishable peaks in the region 2990 – 2850 cm$^{-1}$ with minima and maxima peaks at 2850 and 2922 cm$^{-1}$ respectively corresponding to a C–H stretching vibration of an alkane, and also a vibrational overtone in the region 3100 – 3000 cm$^{-1}$ attributable to a C–H stretch of an aromatic alkene molecule [53]. Thus, the spent catalysts used for single runs has only aromatic sediments deposited on its surface or inside the zeolite channels. However, the spent recycled catalysts contains both unsaturated aliphatic and aromatic compounds which indicates that more unsaturated products are formed at higher repeated runs.

Major differences observed in the spent recycled catalysts after the fourth run for both sets of catalysts include the vibrational bands detected in (i) the region between 3100 – 3000 cm$^{-1}$ with a maxima at

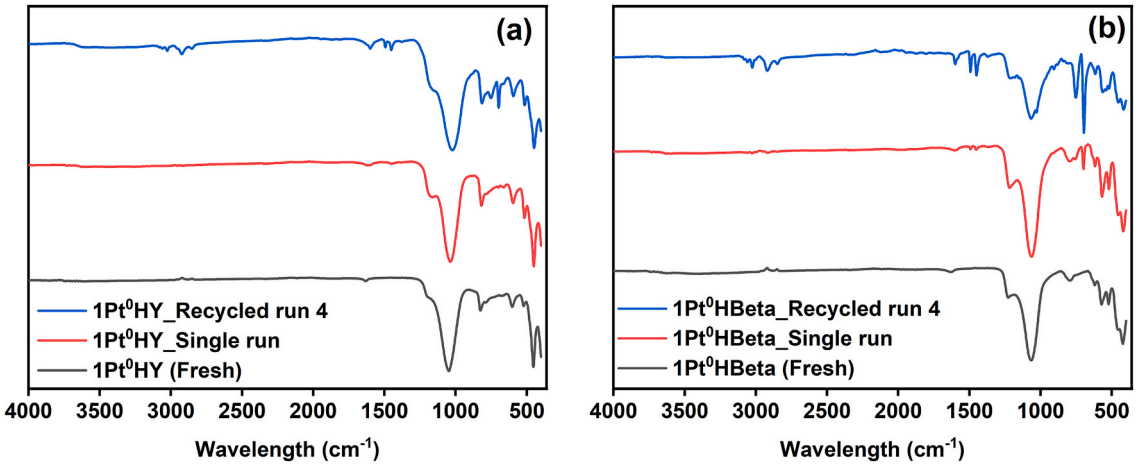


**Fig. 5.** FTIR spectra of fresh and spent catalysts (a) 1Pt$^0$HY (b) 1Pt$^0$HBeta.

3060 and 3025 $cm^{-1}$ attributed to C–H stretching of an alkene or an aromatic compound, (ii) the region between 3000 – 2800 $cm^{-1}$ with a maxima at 2849 and 2927 $cm^{-1}$ corresponding to C–H stretching of an alkane, and (iii) the region between 1625 – 1440 $cm^{-1}$ with a maxima at 1491 and 1451 $cm^{-1}$ assigned to a C=C stretching of an aromatic hydrocarbon. Based on these results, it can be seen that the nature of coke deposited on the spent catalyst after four recycled runs are mainly aromatics which agrees with results reported by Arun et al. [54].

### 3.4. STEM/EDX analysis of spent catalysts

The nature and size of the Pt species, as well as the extent of agglomeration of coke deposits on the metal particles on the zeolite catalysts were obtained via HAADF-STEM measurements. Two sets of spent catalysts (single and recycled run) obtained from hydrocracking reactions under the process conditions: 330 °C, 20 bar, 60 min, and 10:1 polymer:catalyst ratio were analysed. Fresh catalysts were found to have average particle size of 10.3 nm and 1.7 nm for $1Pt^0HY$ and $1Pt^0HBeta$ respectively **(Fig. S1a and b)**. It was observed that the average particle size of Pt on $1Pt^0HY$ increases from 10.3 nm for the fresh catalyst in **Fig. S1a to 12.0** nm for $1Pt^0HY$_Single run **(**Fig. 6**a-b).** The EDX spectra and elemental mapping **(**Figs. 7 and 9**)** of the single run-spent catalysts still revealed the presence of Si, O, Al, and Pt crystals. On the other hand, $1Pt^0HBeta$_Single run still revealed uniformly distributed Pt nanoparticles, appearing as bright spots **(**Fig. 8**a),** but with a longer particle size of 3.1 nm **(**Fig. 8**b)** compared to the fresh $1Pt^0HBeta$ (1.7 nm) **(Fig. S1b)**. The uniform distribution achieved is an indication that the spent catalyst still retains its hydrocracking activity after the first hydrocracking run. However, the increase in the average particle size is due to coke deposition on the catalyst surface as a result of agglomeration of some polymer-derived sediments, which eventually often leads to catalyst deactivation [22].

For the recycled catalysts, the HAADF-STEM micrographs **(**Figs. 10-11**)** and EDX elemental maps **(**Figs. 12-13**)** showed much bigger Pt nanoparticle and an increase in the average particle sizes, obtained as 12.5 nm for $1Pt^0HY$ **(**Fig. 10**b)** and 4.0 nm for $1Pt^0HBeta$ **(**Fig. 11**b)** as the catalysts were being reused for more hydrocracking runs. The increase in the metal particle sizes can be attributed to coking reactions occurring as a result of continuous agglomeration of polymer sediments on the catalysts' surface. The EDX mappings still confirms the presence of Si, O, and Al making up the support and those of the metal crystallite.

### 3.5. Coke distribution via thermal desorption analysis

The spent catalysts were subjected to thermal desorption analysis (TDS) to characterize the coke contents in the catalysts, and to provide an understanding of the process changes and possibly reduce coke formation. Two different heat regimes were employed: (1) the first tube collected after the ramp region (from ambient to 700 °C), and (2) the second tube containing desorbed products in the isothermal region (700 °C) which is left to degrade for 30 min. The desorbed coke products were further analysed with a GC–MS. The obtained spectra of the spent catalysts for both single and recycled runs are shown in **Figs. S5** to **S8**. The $N_2$ desorption results for $1Pt^0HY$_Single run showed that for both stages (ramp and isothermal), the major coke content is single-ring aromatics accounting for at least 79 % at both degradation stages for the used catalysts **(**Table 3**)**. The thermally desorbed hydrocarbon lump distribution profiles of both regions are given in Fig. 14a.

The absence of the more condensed PAHs strongly indicated that the mechanism of coke desorption is governed by the ability of the aromatic rings that are desorbed from the zeolite pores to undergo cracking, rather than dehydrogenation and coupling reactions, leading to the formation of lower molecular weight hydrocarbon molecules (single-ring aromatics) [49]. Other coke compounds include the indenes and naphthalenes accounting for about 6 – 21 % of the total composition. The single-ring aromatics compositions were further deconvoluted into benzene, toluene, EB, styrene, $\alpha$-methyl styrene, and other alkyl-benzene derivatives (Fig. 14a, S5a, S5b). The alkyl-benzenes derivatives and the unsaturated styrene accounts for more than 52 % of the total weight compositions. Interestingly, for the recycled catalyst: $1Pt^0HY$_Recycled run 4 (Fig. 14b, S7), ethylbenzene is present which indicates that the Lewis acid sites (LAS) of the zeolite catalyst which is responsible for the formation of ethylbenzene, a $C_8$ molecule [17] was still active after four repeated runs.

In the case of $1Pt^0HBeta$ catalysts, the carbonaceous deposits obtained were also mainly aromatics. Results obtained showed the species trapped in the spent catalysts consists of single-ring aromatic species (48 % for ramp region, and 86 % for isothermal region). Other coke species include the indenes (9 %), and naphthalenes (4 %) present in roughly same amounts for both regions. About 36 % of fused aromatics are found within the ramp region (Fig. 15a, S6a) while negligible amounts of fused aromatics and higher amounts of single-ring aromatics (87 %) are obtained in the isothermal region (Fig. 15a, S6b). It is likely that these single-ring unsaturated aromatics are formed due to the cracking of the higher aromatics under high temperature conditions during the desorption analysis [49]. The absence of paraffins in the product distribution is due to the enhanced hydrogenation/dehydrogenation ability of the catalyst provided by the metal sites [18,35].

The inset graph in Fig. 15 reveals the single-ring aromatic distribution of the coke species for both regions.

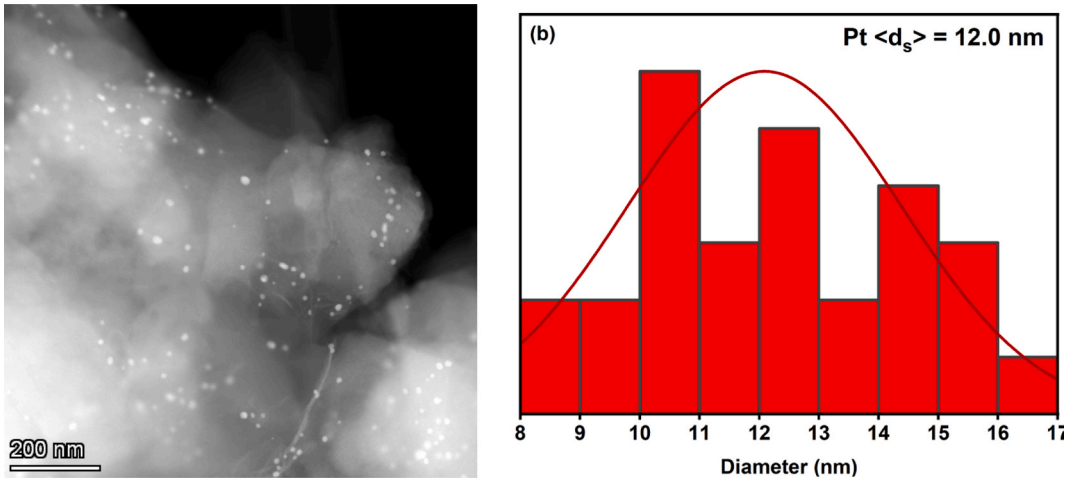


**Fig. 6.** (a) HAADF-STEM micrograph and (b) Pt particle size distribution for spent $1Pt^0HY$ catalyst at 330 °C, 60 min, 20 bar $H_2$, and 10:1 polymer:catalyst ratio for a **single** hydrocracking run. The symbol **< $d_s$ >** denotes the average particle size of platinum (nm).

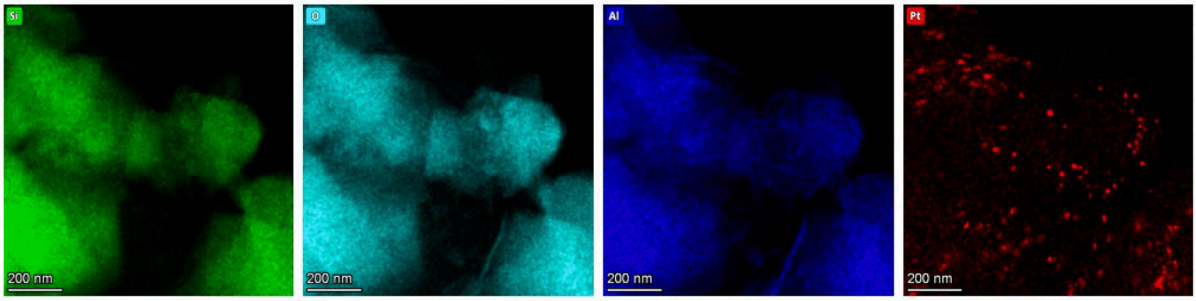


**Fig. 7.** STEM/EDX elemental mapping for Si, O, Al, and Pt of spent $1Pt^0HY$ catalyst at 330°C, 60 min, 20 bar $H_2$, and 10:1 polymer:catalyst ratio for a **single** hydrocracking run.

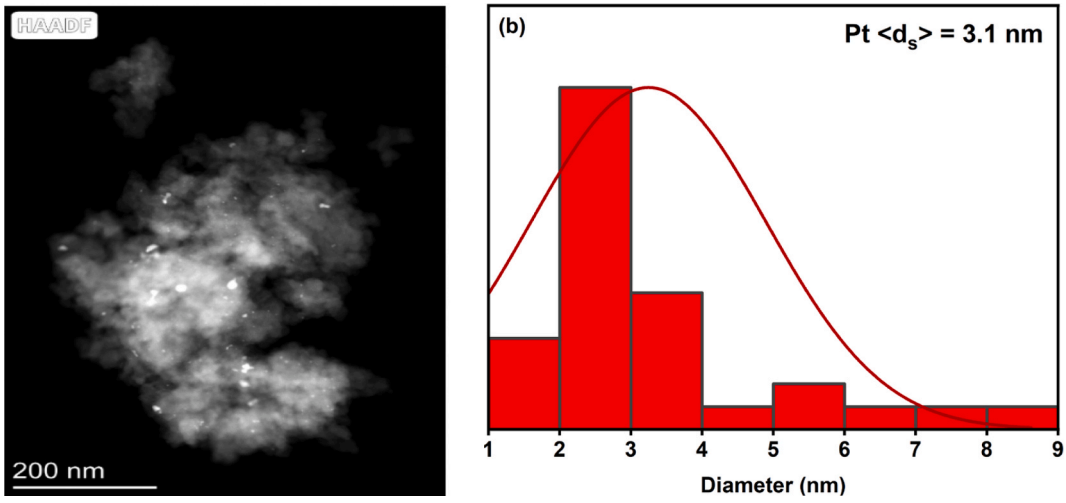


**Fig. 8.** (a) HAADF-STEM micrograph and (b) Pt particle size distribution for spent $1Pt^0HBeta$ catalyst at 330°C, 60 min, 20 bar $H_2$, and 10:1 polymer:catalyst ratio for a **single** hydrocracking run. The symbol **< $d_s$ >** represents the average particle size of platinum (nm).

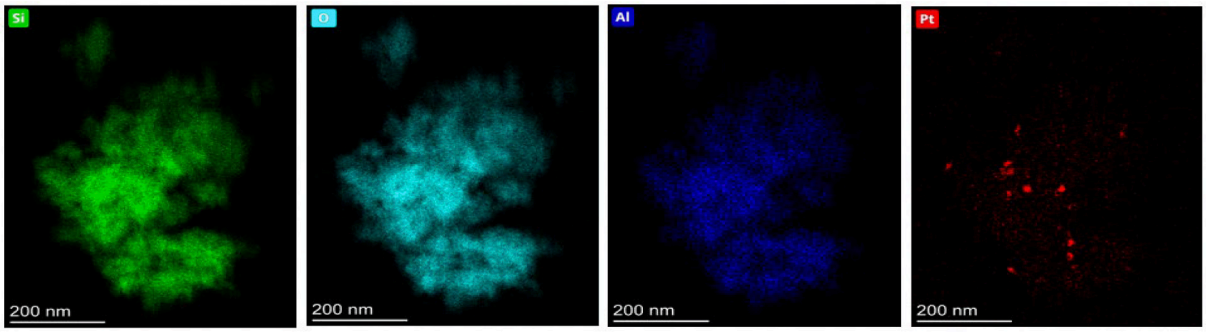


**Fig. 9.** STEM/EDX elemental mapping for Si, O, Al, and Pt of spent $1Pt^0HBeta$ catalyst at 330 °C, 60 min, 20 bar $H_2$, and 10:1 polymer: catalyst ratio for a **single** hydrocracking run.

In the ramp region, the coke deposits consist of the lightest aromatic molecule (benzene) as the major composition (14 %) with an approximate order given as:

***α***-methylstyrene (4 %) < toluene (6 %) < styrene (7 %) < ethylbenzene (8 %) < alkylbenzene (9 %) < benzene (14 %).

However, in the isothermal region, the heavier unsaturated monoaromatic molecule and its derivative (styrene and *α*-methylstyrene) formed the major constituents (43 %) in the order:

Toluene (2 %) < benzene ~ ethylbenzene (13 %) < alkylbenzene ~ ***α***-methylstyrene (15 %) < styrene (28 %).

It is worthy to mention that the evolution of single-ring aromatics at lower temperatures (ramp region) implies that they are mostly present on the external surface of the catalysts as external coke. External coke are often associated with less developed coke deposits with low condensation degrees that requires low temperatures to be decomposed [22], or as a result of PS decomposition that tends to form styrene. On the other hand, the presence of the more developed fused aromatic structures which are degraded at higher temperatures confirm the presence of coke inside the zeolite channels (internal coke) [32].

Interestingly, the TDS-GCMS of the spent recycled catalyst ($1Pt^0HBeta$) shows mainly monoaromatics (~95 %) with negligible amounts of cycloalkanes (~1%), (indanes (~1%), naphthalenes (3 %), and no amounts of fused aromatics (Fig. 15b), spectra in **Fig. S8a-b).** This implies that continuous use of the zeolite catalysts resulted in

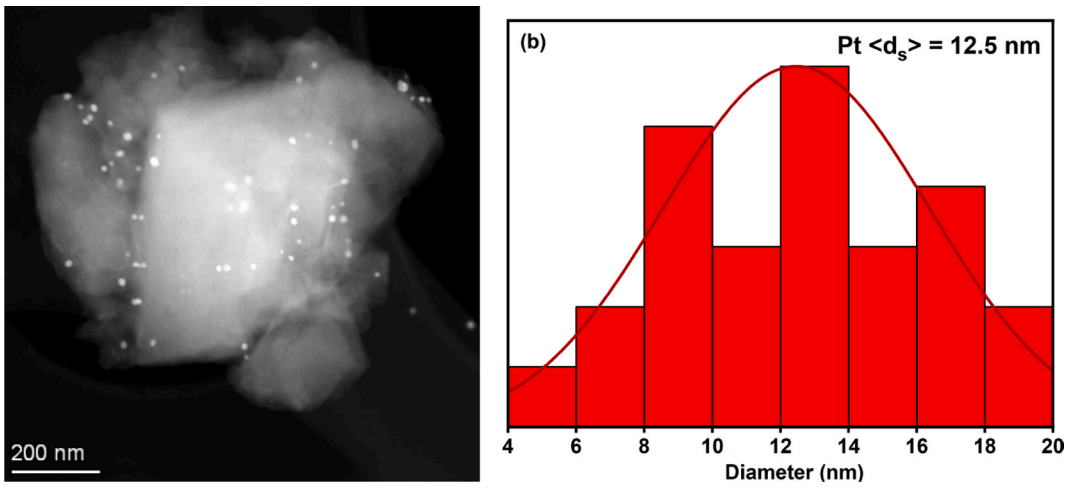


**Fig. 10.** (a) HAADF-STEM micrograph and (b) Pt particle size distribution for spent $1Pt^0HY$ catalyst at 330 °C, 60 min, 20 bar $H_2$, and 10:1 polymer:catalyst ratio after **four recycle** hydrocracking runs. The symbol < $\mathbf{d_s}$ > denotes the average particle size of platinum (nm).

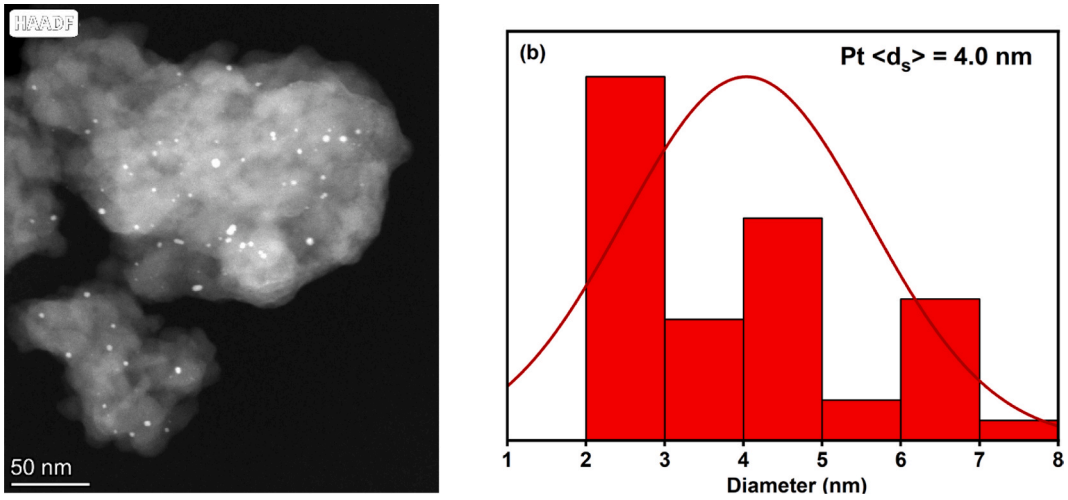


**Fig. 11.** (a) HAADF-STEM micrograph and (b) Pt particle size distribution for spent $1Pt^0HBeta$ catalyst at 330 °C, 60 min, 20 bar $H_2$, and 10:1 polymer:catalyst ratio after **four recycle** hydrocracking runs. The symbol < $\mathbf{d_s}$ > represents the average particle size of platinum (nm).

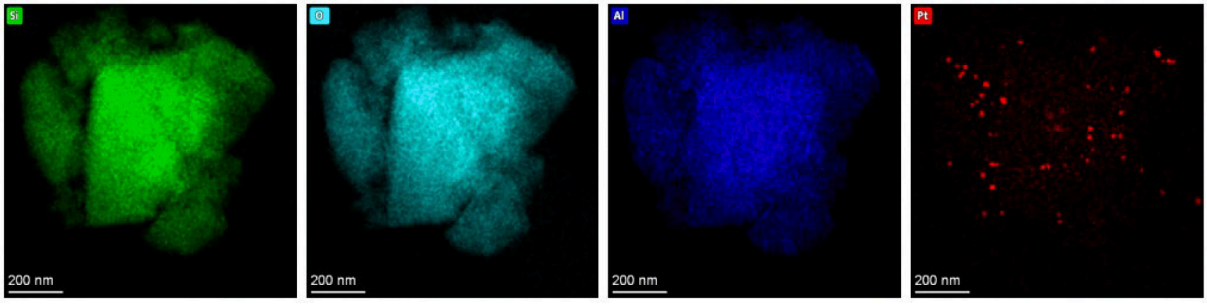


**Fig. 12.** STEM/EDX elemental mapping for Si, O, Al, and Pt of spent $1Pt^0HY$ catalyst at 330 °C, 60 min, 20 bar $H_2$, and 10:1 polymer:catalyst ratio after **four recycle** hydrocracking runs.

decreased catalytic activity. This, coupled with the high temperature desorption analysis has led to rapid cracking of the tri-aromatics into mono-substituted aromatic products. The single-ring aromatic distribution of the thermally desorbed recycled catalyst for both ramp and isothermal region as shown in Fig. 15b highlights a relatively higher amount of unsaturated styrene molecule (69 %) in the isothermal region and low amounts of the lower molecular weight monoaromatics. Thus, TDS-GCMS analysis of the spent catalysts further confirms the FTIR results that the coke contents are mainly aromatics and are present both inside the zeolitic channels and on the outer surface of the catalyst.

## 4. Conclusion

A comprehensive study of coke deposited on spent zeolite catalysts

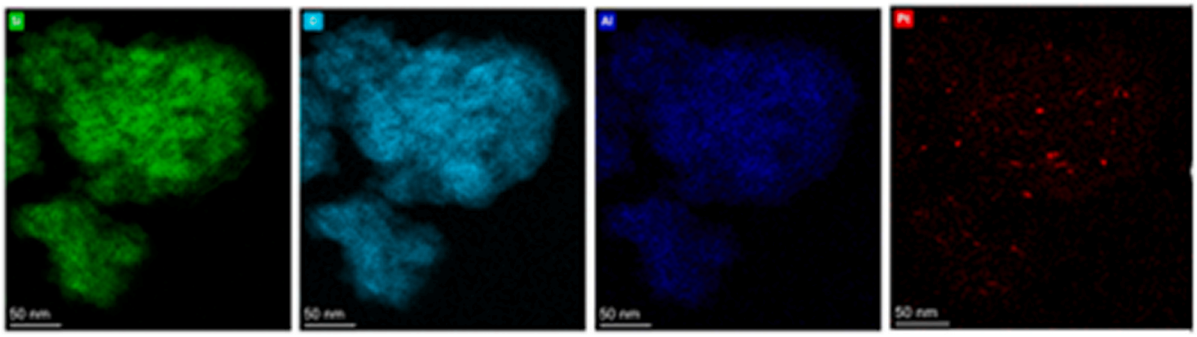


**Fig. 13.** STEM/EDX elemental mapping for Si, O, Al, and Pt of spent $1Pt^0HBeta$ catalyst at 330 °C, 60 min, 20 bar $H_2$, and 10:1 polymer:catalyst ratio after **four recycle** hydrocracking runs.

**Table 3**
Coke desorption composition of spent catalysts.

| Desorbed catalysts | Composition (wt.%) | | |
|---|---|---|---|
| | Single-ring aromatics | Indenes | Naphthalenes |
| $1Pt^0HY$_Single run (Ramp region) | 100 | – | – |
| $1Pt^0HY$_Single run (Isothermal region) | 79.4 | 15.3 | 5.3 |
| $1Pt^0HY$_Recycled run 4 (Ramp region) | 93.3 | 2.9 | 3.8 |
| $1Pt^0HY$_Recycled run 4 (Isothermal region) | 93.5 | 4.1 | 2.4 |

for hydrocracking of post-consumer expanded PS waste has been carried out. The thermal degradation profiles provided information on the amounts of chemical species and coke compounds present in the spent catalysts after different hydrocracking process conditions. The amount and nature of coke was found to depend on the operating conditions, as well as the nature of the acid sites of the zeolite. Coke content was found to decrease as reaction time, hydrogen pressure, and temperature increases, while an increase in the polymer:catalyst ratio increases the coke content as lower amount of catalyst relative to the polymer feedstock (15:1) causes condensation of coke deposits on the zeolite pores and surface leading to sintering of Pt particles.

Coke analysis shows quite similar amounts with same hydrocracking feedstock and operating conditions for the HY catalysts. However, for both HY and HBeta catalysts, the differences observed in those of the single runs relative to the repeated runs, parent zeolite (HY and HBeta), as well as the oxidised Pt-doped (1PtHY and 1PtHBeta) strongly indicates that the nature and amount of coke in PS hydrocracking with zeolite catalysts largely depends on the availability and size of both supercage and β-cage pores, as well as the nature and strength of the acid sites.

FTIR was used to identify the different functional groups present in both spent and unspent catalysts, while TDS-GC–MS helped to understand the nature and content of the coke. FTIR and TDS-GCMS of the solid residue revealed the coke compositions as mainly aromatics, formed as a result of condensation reactions of hydrocracking products and are deposited both inside the zeolite channels and on the outer surface of the catalysts.

We have provided a systemic approach to understand the dynamics of coke deposition of some zeolite catalysts used in the hydrocracking of polystyrene wastes. This is expected to provide information that will promote the design of active and sustainable catalysts with sufficient thermal stability, appropriate porous structures with high resistance to both sintering and coking. This will further help in the development of low cost and regenerable catalysts towards the thermochemical conversion of waste plastics to desired products.

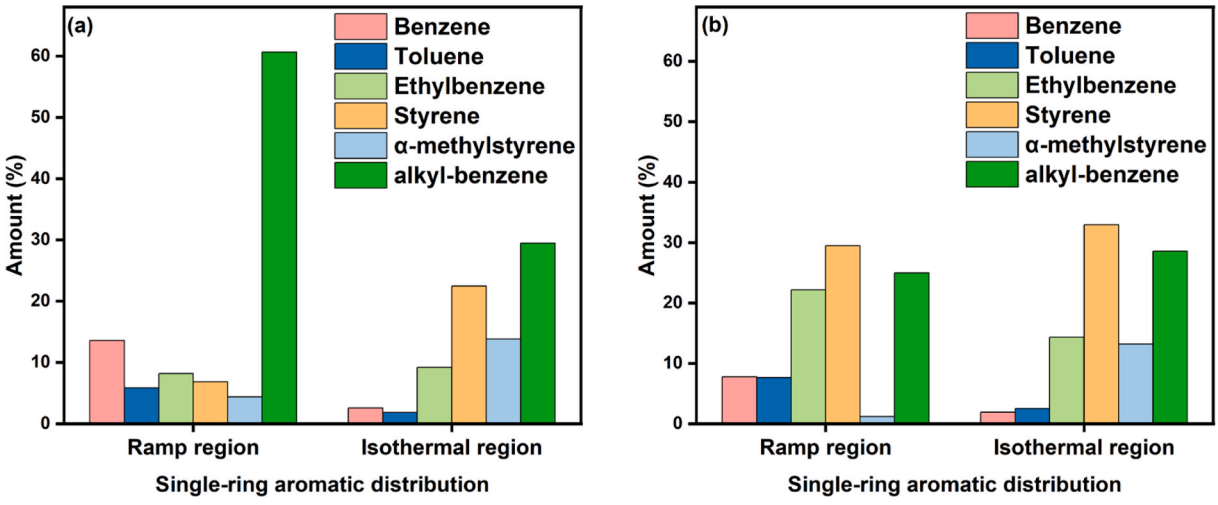


**Fig. 14.** Single-ring aromatic composition of desorbed spent catalyst (a) $1Pt^0HY$_Single run (b) $1Pt^0HY$_Recycled run 4.

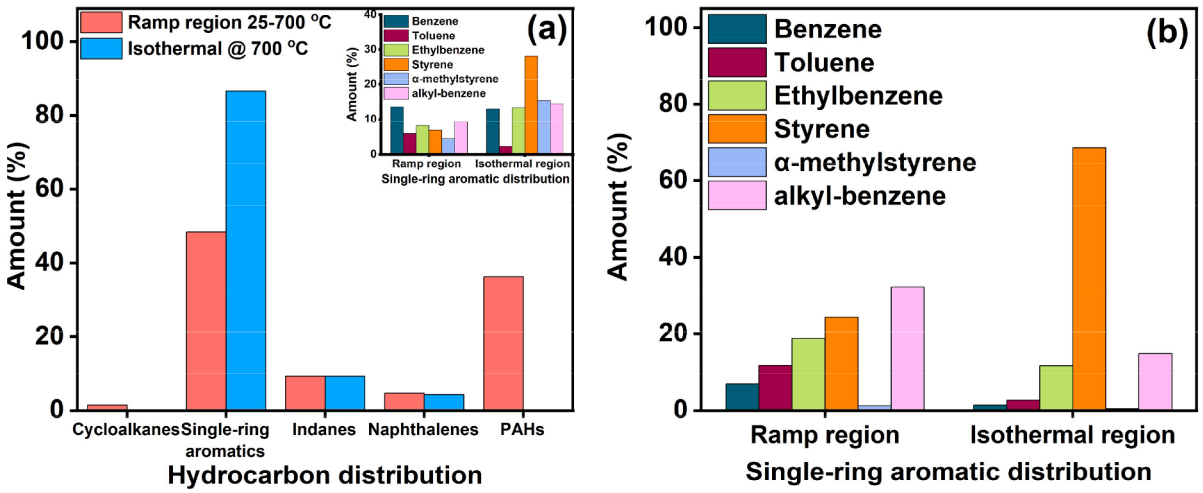


**Fig. 15.** Thermal desorption hydrocarbon distribution profile for spent HBeta catalysts with different heat regions: ramp from 25 – 700 °C, isothermal at 700 °C for 30 min (a) $1Pt^0$ HBeta_Single run, (b) $1Pt^0$ HBeta_Recycled run 4 (For interpretation of the references to colour in this figure legend, the reader is referred to the web version of this article.)

## CRediT authorship contribution statement

**Olajumoke Alabi-Babalola:** Writing – original draft, Writing – review & editing, Methodology, Formal analysis, Data curation. **Vijayalakshmi Thangaraj:** Writing – review & editing, Methodology, Formal analysis, Data curation. **Nasser Alqahtani:** Writing – review & editing, Resources, Methodology, Formal analysis. **Hubertus Warsahartana:** Writing – review & editing, Resources, Methodology, Formal analysis. **Matthew Smith:** Writing – review & editing, Resources, Methodology, Formal analysis, Data curation. **Edidiong Asuquo:** Writing – review & editing, Validation, Project administration, Methodology, Formal analysis, Conceptualization. **Carmine D'Agostino:** Writing – review & editing, Supervision, Resources, Project administration, Methodology, Formal analysis. **Arthur Garforth:** Writing – review & editing, Validation, Supervision, Resources, Project administration, Methodology, Investigation, Funding acquisition, Formal analysis, Data curation, Conceptualization.

## Declaration of competing interest

The authors declare that they have no known competing financial interests or personal relationships that could have appeared to influence the work reported in this paper.

## Acknowledgements

This work is supported by Olajumoke Alabi-Babalola's PhD sponsor: The Petroleum Technology Development Fund (PTDF), Nigeria. The authors would like to thank the Henry Royce Institute for Advanced Materials for providing access to the Electron Microscopy Suite funded by EPSRC grants EP/R00661X/1, EP/S019367/1, EP/P025021/1 and EP/P025498/1, and Verder Scientific UK Ltd for access to the BELCAT II / TPD / TPO / TPR instrument. In addition, the authors also acknowledge the support of Prof. Bart E. van Dongen and Dr. Stephen Boult in the Department of Earth and Environmental Sciences, School of Natural Science, University of Manchester for their assistance in the analysis of some catalysts reported in this work.

## Appendix A. Supplementary data

Supplementary data to this article can be found online at https://doi.org/10.1016/j.fuel.2025.136089.

## Data availability

Data will be made available on request.

## References

[1] OECD, *Global plastic waste set to almost triple by 2060*. 2022.
[2] Garforth AA, et al. *Feedstock recycling of polymer wastes*. Curr. Opin. Solid State Mater. Sci. 2004;8(6):419–25.
[3] Aguado, J. and D.P. Serrano, *Feedstock recycling of plastic wastes*. 2007: Royal society of chemistry.
[4] Davidson MG, Furlong RA, McManus MC. *Developments in the life cycle assessment of chemical recycling of plastic waste–a review*. J. Clean. Prod. 2021;293:126163.
[5] Akah, A., et al. *Enhanced feedstock recycling of post-consumer plastic*. in *ICheaP12*. 201AIDIC.
[6] Zhao X, et al. *Plastic waste upcycling toward a circular economy*. Chem. Eng. J. 2022; 428:131928.
[7] Al-Salem S, et al. *A review on thermal and catalytic pyrolysis of plastic solid waste (PSW)*. J. Environ. Manage. 2017;197:177–98.
[8] Budsaereechai S, Hunt AJ, Ngernyen Y. *Catalytic pyrolysis of plastic waste for the production of liquid fuels for engines*. RSC Adv. 2019;9(10):5844–57.
[9] Ding W, Liang J, Anderson LL. *Hydrocracking and hydroisomerization of high-density polyethylene and waste plastic over zeolite and silica– alumina-supported Ni and Ni–Mo sulfides*. Energy Fuel 1997;11(6):1219–24.
[10] Hauli L, Wijaya K, Syoufian A. *Hydrocracking of LDPE plastic waste into liquid fuel over sulfated zirconia from a commercial zirconia nanopowder*. Orient. J. Chem. 2019; 35(1):128–33.
[11] Kremer I, et al. *Catalytic pyrolysis of mechanically non-recyclable waste plastics mixture: Kinetics and pyrolysis in laboratory-scale reactor*. J. Environ. Manage. 2021; 296:113145.
[12] Alabi-Babalola O, Aransiola E, Shittu T. *A Study on the Optimization and Adsorption Capacity of Activated Carbon Produced from polyvinyl Chloride (PVC) Wastes*. Ife Journal of Technology 2019;26(1):34–46.
[13] Adrados A, et al. *Pyrolysis of plastic packaging waste: a comparison of plastic residuals from material recovery facilities with simulated plastic waste*. Waste Manag. 2012;32 (5):826–32.
[14] Weitkamp J. *Catalytic hydrocracking—mechanisms and versatility of the process*. ChemCatChem 2012;4(3):292–306.
[15] Bin Jumah A, et al. *Kinetic modeling of hydrocracking of low-density polyethylene in a batch reactor*. ACS Sustain. Chem. Eng. 2021;9(49):16757–69.
[16] Venkatesh KR, et al. *Hydrocracking and hydroisomerization of long-chain alkanes and polyolefins over metal-promoted anion-modified zirconium oxides*. Energy Fuel 1996; 10(6):1163–70.
[17] Fuentes, E., et al. Polystirene Hydrocracking in Solution over Bifunctional Catalysts. in Proceedings of the 6th international symposium on feedstock recycling of polymeric materials. Toledo, Spain. 2011.
[18] Vance BC, et al. *Single pot catalyst strategy to branched products via adhesive isomerization and hydrocracking of polyethylene over platinum tungstated zirconia*. Appl Catal B 2021;299:120483.
[19] Fuentes-Ordonez EG, et al. *Transport phenomena in catalytic hydrocracking of polystyrene in solution*. Ind. Eng. Chem. Res. 2013;52(42):14798–807.
[20] Liu, S., et al., *Plastic waste to fuels by hydrocracking at mild conditions*. Science Advances, 2021. **7**(17): p. eabf8283.
[21] Francis J, et al. *Design of improved hydrocracking catalysts by increasing the proximity between acid and metallic sites*. Appl. Catal. A 2011;409:140–7.

[22] Trueba D, et al. *Product composition and coke deposition in the hydrocracking of polystyrene blended with vacuum gasoil*. Fuel Process. Technol. 2021;224:107010.
[23] Kubička D, et al. *Ring opening of decalin over zeolites: II. activity and selectivity of platinum-modified zeolites*. J. Catal. 2004;227(2):313–27.
[24] Fuentes-Ordóñez EG, et al. *Mechanism and kinetics in catalytic hydrocracking of polystyrene in solution*. Polym. Degrad. Stab. 2016;124:51–9.
[25] Boerefijn R, Gudde N, Ghadiri M. *A review of attrition of fluid cracking catalyst particles*. Adv. Powder Technol. 2000;11(2):145–74.
[26] Werther J, Reppenhagen J. *Catalyst attrition in fluidized-bed systems*. AIChE J 1999; 45(9):2001–10.
[27] Bartholomew CH. *Mechanisms of catalyst deactivation*. Appl. Catal. A 2001;212 (1–2):17–60.
[28] Guisnet, M. and F.R. a Ribeiro, *Deactivation and regeneration of zeolite catalysts*. 2011.
[29] Tailleur RG. *Hydrogenation and hydrodesulfurization in gas phase of light hydrocarbons from hydrocracking, desulfurization and delayed coking*. I catalyst deactivation Chemical Engineering Science 2019;210:115195.
[30] Al-Khattaf S, et al. *The effect of coke deposition on the activity and selectivity of the HZSM-5 zeolite during ethylbenzene alkylation reaction in the presence of ethanol*. Cat. Sci. Technol. 2014;4(4):1017–27.
[31] He S, et al. *Characterization of coke deposited on spent catalysts for long-chain-paraffin dehydrogenation*. Chem. Eng. J. 2010;163(3):389–94.
[32] Fals J, et al. *A comprehensive study of product distributions and coke deposition during catalytic cracking of vacuum gas oil over hierarchical zeolites*. Heliyon 2023;9(4).
[33] Rodríguez E, et al. *Lessening coke formation and boosting gasoline yield by incorporating scrap tire pyrolysis oil in the cracking conditions of an FCC unit*. Energ. Conver. Manage. 2020;224:113327.
[34] Gutiérrez A, et al. *Role of acidity in the deactivation and steady hydroconversion of light cycle oil on noble metal supported catalysts*. Energy Fuel 2011;25(8):3389–99.
[35] Chen C, et al. *Enhanced performance in catalytic combustion of toluene over mesoporous Beta zeolite-supported platinum catalyst*. Appl Catal B 2013;140:199–205.
[36] Larsen G, et al. *A study of platinum supported on tungstated zirconia catalysts*. Appl. Catal. A 1996;139(1–2):201–11.
[37] Gutiérrez A, et al. *Effect of pressure on the hydrocracking of light cycle oil with a Pt–Pd/HY catalyst*. Energy Fuel 2012;26(9):5897–904.
[38] Paulik J, Paulik F, Czaran E. *The thermal decomposition of platinum tetrammine chloride*. Anal. Chim. Acta 1978;101(2):409–12.
[39] Venezia AM. *X-ray photoelectron spectroscopy (XPS) for catalysts characterization*. Catal. Today 2003;77(4):359–70.
[40] Fairley N, et al. *Systematic and collaborative approach to problem solving using X-ray photoelectron spectroscopy*. Appl. Surf. Sci. Adv. 2021;5:100112.
[41] Khalfaoui M, et al. *New theoretical expressions for the five adsorption type isotherms classified by BET based on statistical physics treatment*. J. Colloid Interface Sci. 2003; 263(2):350–6.
[42] Sato K, et al. *Role of HY zeolite mesopores in hydrocracking of heavy oils*. J. Catal. 2001;200(2):288–97.
[43] Bhatia S, Beltramini J, Do D. *Temperature programmed analysis and its applications in catalytic systems*. Catal. Today 1990;7(3):309–438.
[44] bin Jumah, A., A.A. Tedstone, and A.A. Garforth, *Hydrocracking of virgin and post-consumer polymers*. Microporous and Mesoporous Materials, 2021. **315**: p. 110912.
[45] Bastl Z, Kubelková L, Nováková J. *XPS study of Pt ammine decomposition in K faujasites: Comparison with bulk behavior*. Zeolites 1997;19(4):279–87.
[46] Wagner, C., et al., *NIST X-ray photoelectron spectroscopy database, NIST standard reference database 20, version 3.4 (Web version)*. US Department of Commerce, 2003. **1**.
[47] Jackson S, et al. *Supported metal catalysts: preparation, characterization, and function: I. Preparation and physical characterization of platinum catalysts*. J. Catal. 1993;139 (1):191–206.
[48] Paparazzo E. *On the interpretation of XPS spectra of metal (Pt, Pt–Sn) nanoparticle/ graphene systems*. Carbon 2013;63:578–81.
[49] Sanapur G, et al. *Thermal desorption and characterization of carbonaceous deposits in Mo/HZSM-5 catalyst*. J. Anal. Appl. Pyrol. 2019;138:22–8.
[50] Rodríguez E, et al. *Modeling of hydrotreating catalyst deactivation for heavy oil hydrocarbons*. Fuel 2018;225:118–33.
[51] Huang J, et al. *Chemical recycling of plastic waste for sustainable material management: a prospective review on catalysts and processes*. Renew. Sustain. Energy Rev. 2022;154:111866.
[52] Movasaghi Z, Rehman S, ur Rehman DI. *Fourier transform infrared (FTIR) spectroscopy of biological tissues*. Appl. Spectrosc. Rev. 2008;43(2):134–79.
[53] Juybar M, Khorrami MK, Garmarudi AB. *FTIR/PLS and SVM multivariate calibrations to determination of the coke amount into the deactivated catalysts and the product of the methanol to gasoline conversion*. Infrared Phys. Technol. 2020;105: 103229.
[54] Devaraj A, et al. *Discerning the location and nature of coke deposition from surface to bulk of spent zeolite catalysts*. Sci. Rep. 2016;6(1):37586.